Chinese Chemical Letters 31 (2020) 755–758

Contents lists available at ScienceDirect

Chinese Chemical Letters

journal homepage: www.elsevier.com/locate/cclet

Communication

Conjugated polymer nanoparticles as fluorescence switch for selective cell imaging

Ke Peng[a,b], Fengting Lv[a,*], Huan Lu[a], Jianwu Wang[a,b], Hao Zhao[a,b], Libing Liu[a], Shu Wang[a,b]

[a] Beijing National Laboratory for Molecular Sciences, Key Laboratory of Organic Solids, Institute of Chemistry, Chinese Academy of Sciences, Beijing 100190, China
[b] College of Chemistry, University of Chinese Academy of Sciences, Beijing 100049, China

ARTICLE INFO

Article history:
Received 10 August 2019
Received in revised form 9 September 2019
Accepted 10 September 2019
Available online 11 September 2019

Keywords:
Electrostatic complex nanoparticles
Conjugated polymers
Fluorescence switch
Cell imaging
Selective cell lighting up

ABSTRACT

Fluorescence switch plays a vital role in bioelectronics and bioimaging. Herein, we presented a new kind of facile electrostatic complex nanoparticles (ECNs) for fluorescence switching in cells and marking of individual cell. The ECNs were prepared by mixing positively charged poly(6-(2-(thiophen-3-yl)ethoxy) hexyl trimethylammonium bromide) (PT) and negatively charged diarylethene sodium salt (DAE-COONa). DAE-COONa is a photoswitchable molecule which can be transformed between the ring-closed form and ring-open form under the irradiation of UV or visible light. The closed-form of DAE-COONa can efficiently quench the fluorescence of PT through intermolecular energy transfer, while the open form of DAE-COONa does not influence the emission of PT. Thus, the fluorescence of ECNs can be modulated by light irradiation, and the ECNs with good fluorescence switching performance have been employed for fluorescence imaging and individual cell lighting up process successfully. We demonstrate that the electrostatic complex strategy provides a facile method to construct fluorescence switch for selective cell marking and imaging applications.

Fluorescence imaging is an important technique for studying cell structures and biological events, such as cell-matrix adhesion structure [1], membrane dynamics [2], drug delivery process [3], antibody-biological structure interactions [4] and cell morphological changes [5]. Since light controlled fluorescence switching process contains fluorescence "on" and "off" state, the real signal of biosamples can be distinguished from background signal and autofluorescence, which greatly improves signal-to-noise ratio for higher imaging resolution [6]. Furthermore, fluorescence switching process can also be applied in selectively lighting up specific region, which is useful in super resolution fluorescence microscopy to overcome diffraction limit [7,8]. Thus, constructing light controlled fluorescence switching system is of great importance due to its broad applicability. Photochromic molecules are necessary components for a fluorescence switching system. They can transform between two states by irradiation with light of different wavelengths. The most widely used photochromic molecules in fluorescence switch are azobenzene [9,10], spiropyran [11–13], diarylethene [14–16] and Sternhouse adduct [17]. The closed states of azobenzenes, spiropyrans and Sternhouse adducts after irradiation are not thermally stable [17,18], which will spontaneously recover to their original states without light irradiation. On the contrary, both ring-open and ring-closed forms of diarylethenes are relatively thermostable, hence, diarylethenes are considered as a better choice for a reliable fluorescence switch. To acquire a good performance of fluorescence switching system, bright and stable fluorophores are also in great demand. Recently, plenty of fluorophores were developed on fluorescence switch, including fluorescent proteins [19,20], small organic dyes [21–24], QDs [25–28] and conjugated polymers [29–31]. Among them, conjugated polymers (CPs) attract much more attention due to their photostability and bright fluorescence, good biocompatibility [32], which makes CPs as preferable choice for constructing fluorescence switching systems.

Construction methods of fluorescence switching system mainly fall into two classifications, the covalent binding and noncovalent mixing. Covalent binding method eliminates undesired leakage, but complicated synthetic modifications are needed [29]. In non-covalent mixing method, normal strategy is nanoprecipitation [31,33], in which hydrophobic fluorophores and hydrophobic photochromic molecules are encapsulated together by an

* Corresponding author.
E-mail address: lvft@iccas.ac.cn (F. Lv).

https://doi.org/10.1016/j.cclet.2019.09.019
1001-8417/

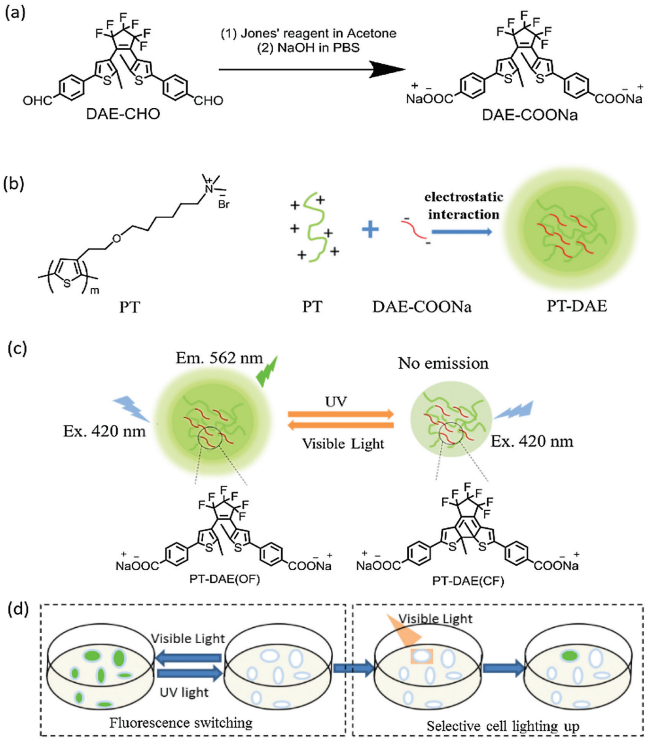

Scheme 1. (a) The synthetic route of DAE-COONa. (b) The positively charged PT interacts with negatively charged DAE-COONa to form PT-DAE ECN. (c) The fluorescence switching process of PT-DAE ECN and the photoswitching process of DAE-COONa, where OF means open-form and CF means closed-form. (d) The fluorescence switching process of ECN on cells and lighting up process on selected cell.

amphiphilic polymers, such as poly(styrene-*g*-ethylene oxide) or poly(styrene-*co*-maleic anhydride) [34]. Better switch efficiency is realized due to the easily adjustable ratio of photochromic molecules in this method rather than covalent binding method. However, this method still involves multiple components leading to complicated preparation process towards making nanoparticles. Electrostatic complex nanoparticles (ECNs) prepared through simply mixing two oppositely charged components have been used successfully in tumor imaging [35], anti-cancer [36] and anti-bacteria applications [37]. As a simple method of noncovalent mixing, electrostatic complex may provide an easy approach to construct fluorescence switches.

Herein, an easily accessible ECN was fabricated through simply mixing two oppositely charged components together, which were negatively charged diarylethene sodium salt (DAE-COONa, structure shown in Scheme 1a) and positively charged poly(6-(2-(thiophen-3-yl)ethoxy)hexyl trimethylammonium bromide) (PT, structure shown in Scheme 1b). As demonstrated in Scheme 1c, the ECNs present bright fluorescence due to the strong emission of PT, after 30 s UV irradiation, DAE-COONa transforms to the closed form, which efficiently quench the fluorescence of PT. This process can be reversed by visible light irradiation for several minutes to turn the closed form of DAE-COONa into its open form again realizing fluorescence switching. This nanoparticle exhibits improved fluorescence switching ability and distinct selective cell lighting up ability as shown in Scheme 1d.

Table 1
DLS size and zeta potential (ζ) of PT and DAE-COONa, and the absolute fluorescence quantum yield of PT-DAE ECs.

Sample	PT-DAE-1	PT-DAE-2	PT-DAE-3	PT-DAE-4	PT	DAE-COONa
Size (nm)	1102.1	1048.2	285.6	850.1	7.2	6.4
ζ (mV)	−22.6	−25.1	−31.0	−34.5	17.3	−40.4
OF (%)	3.13	2.59	2.34	2.70	/	/
CF (%)	0.39	0.69	0.99	0.61	/	/

Fig. 1 describes that the fluorescence spectrum of PT (emission range 500-750 nm) overlaps well with the absorbance spectrum of closed form of DAE-COONa, so an efficient fluorescence quenching of PT is expected due to the well-overlapped spectrum. In addition, the absorbance spectrum of open-form of DAE-COONa has no overlap with the fluorescence spectrum of PT, thus no fluorescence quenching is expected. As shown in Scheme 1c, the closed and open-form of DAE-COONa can be controlled by UV and visible light irradiation [14], which means the fluorescence of PT-DAE pair can be modulated through light irradiation. Moreover, the energy transfer process becomes easier when donor and acceptor get closer [36], so the compact electrostatic complex nanoparticles, which were formed by positively-charged PT and the negatively-charged DAE-COONa, can efficiently enhance the energy transfer process from PT to DAECOONa.

To optimize the ratio of PT and DAE-COONa for fluorescence switching, four batches of electrostatic complex nanoparticles of PT and DAE-COONa (PT-DAE-1, PT-DAE-2, PT-DAE-3 and PT-DAE-4) were prepared. In these four batches of electrostatic complexes (ECs), the concentration of PT was kept as 32 μmol/L, while the concentrations of DAE-COONa were 64 μmol/L, 128 μmol/L, 256 μmol/L, 512 μmol/L for PT-DAE-1, PT-DAE-2, PT-DAE-3 and PT-DAE-4, respectively. The hydrodynamic diameters of PT-DAE-1, PT-DAE-2 and PT-DAE-4 in DLS measurements were given in Fig. S1 (Supporting information), and summarized in Table 1. The hydrodynamic diameters of PT-DAE-3 was around 300 nm, which was smaller than other three electrostatic complexes. As shown in Fig. 2, TEM images showed uniform particle sizes of PT-DAEs and collaborate with the diameter obtained in DLS measurements. Fig. 2e and f showing little aggregation of pure DAE-COONa and PT proved that aggregation did not occur before PT was mixed with DAE-COONa. From TEM it was clear that the diameter of PT-DAE-3

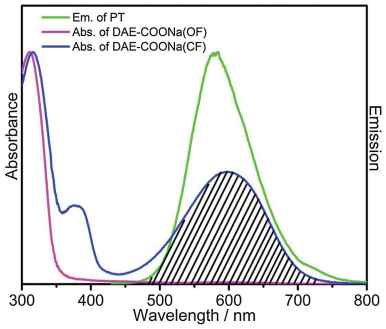

Fig. 1. The emission spectrum of PT and the absorbance of DAE-COONa (open-form, OF) or DAE-COONa (colesed-form, CF).

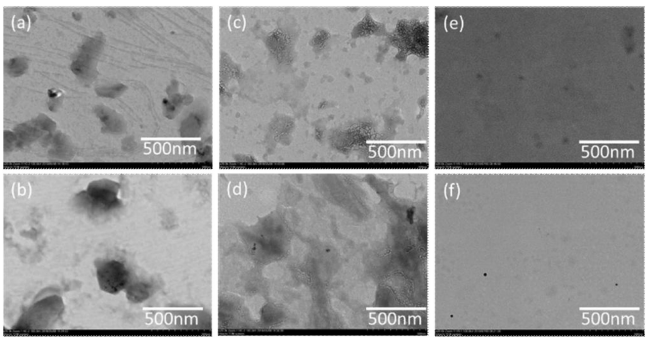

Fig. 2. The TEM images of PT-DAE-1, 2, 3, 4 (a-d), DAE-COONa (e) and PT (f).

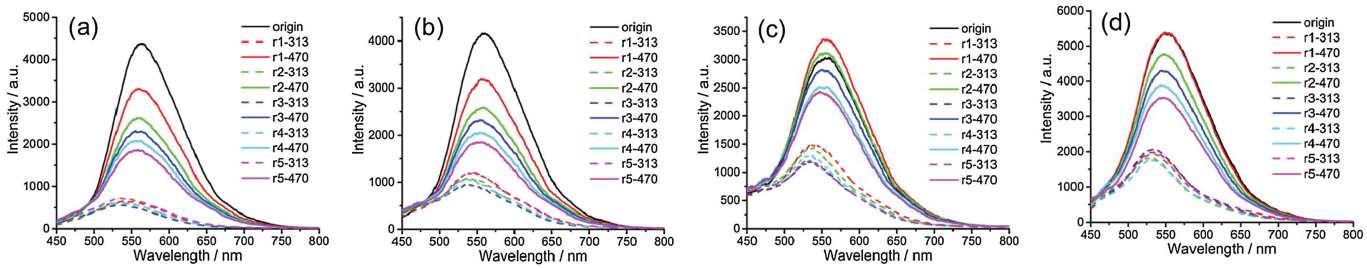

Fig. 3. Fluorescence switching cycles of four electrostatic complexes (PT-DAE ECs): PT-DAE-1 (a), PT-DAE-2 (b), PT-DAE-3 (c) and PT-DAE-4 (d). 'rx'(x = 1-5) means cycle number is x, '313' means the exact wavelength used for irradiation, '470' means the irradiation wavelength is longer than 470 nm. Excitation wavelength is 420 nm.

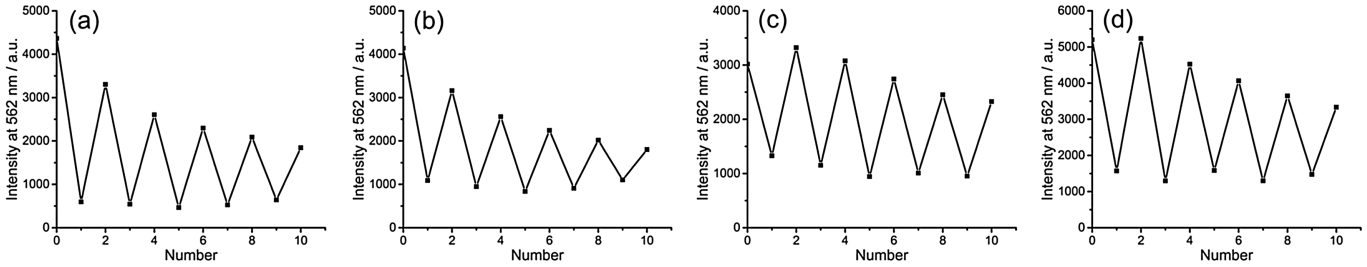

Fig. 4. Fluorescence switching cycles at the maximum fluorescence peak at 562 nm for PT-DAE-1 (a), PT-DAE-2 (b), PT-DAE-3 (c) and PT-DAE-4 (d), respectively.

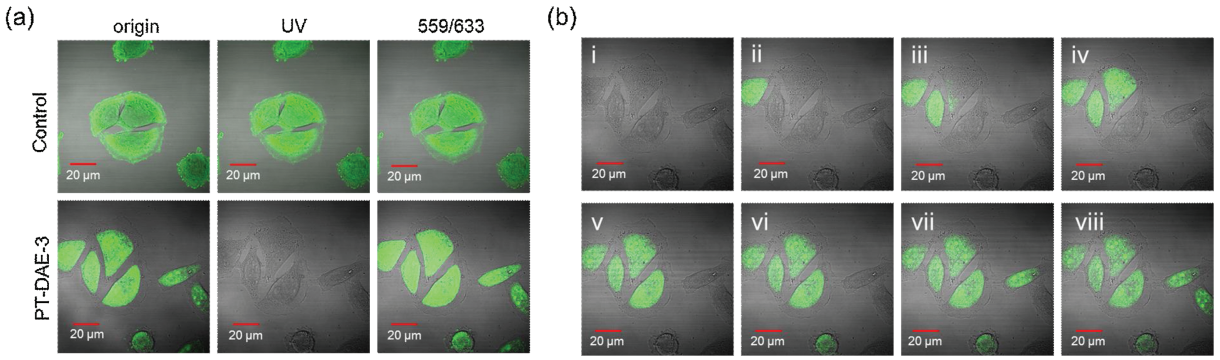

Fig. 5. Fluorescence switching experiments on (a) whole MCF-7 cells. Cells were incubated with PT (control group) or PT-DAE-3 for 4 h, respectively. UV light and 559/633 nm laser were given by CLSM. (b) Selective cell fluorescence lighting up process on MCF-7 cells. Cells were irradiated by small region 559/633 nm laser of CLSM one by one (from i to viii). PT-DAE-3 was prepared by mixing PT (32 μmol/L) and DAE (256 μmol/L) to form electrostatic complex nanoparticles.

was less than other ECs, which was in accordance with the DLS results. The size of PT-DAE-3 was less than 100 nm, but PT-DAE-1, PT-DAE-2 and PT-DAE-4 were mostly larger than 300 nm as observed from TEM images. In the case of PT-DAE-1 and PT-DAE-2, PT concentration was relative high and DAE-COONa concentration was low, which lead to form a relatively loose aggregate. Similarly, the concentration of DAE-COONa was high in PT-DAE-4, which also influence the formation of the compact PT/DAE aggregation. PT-DAE-3 had a balanced concentration of PT and DAE-COONa, therefore, it presented a smaller size due to the formation of the compact nanoparticles.

The zeta potential of PT-DAEs, PT and DAE-COONa were shown in Table 1 to further demonstrate the electrostatic complex formed between PT and DAE-COONa. Zeta potential of PT was positively charged surface with zeta potential of 17.3 mV and DAE-COONa was negatively charged with zeta potential of −40.4 mV. PT-DAE-1, PT-DAE-2, PT-DAE-3 and PT-DAE-4 were found to have gradually decreased negative zeta potential but not exceeded −40.4 mV, which further proved the formation of PT-DAE electrostatic complex.

The absolute quantum yields of PT-DAE-1, PT-DAE-2, PT-DAE-3 and PT-DAE-4 were tested before and after UV irradiation to confirm energy transfer process. As Table 1 tells, the closed form of PT-DAE display much lower fluorescence quantum yield than their open form electrostatic complexes. The absolute quantum yield measurements proved that energy could only be transferred from PT to closed form of DAE-COONa rather than open-form of DAE-COONa. As expected, the emission of PT can only be quenched by closed-form of DAE-COONa rather than the open-form one.

The fluorescence switch performance of all these electrostatic complexes were tested separately. As shown in Fig. 3, they all showed good fluorescence switching behavior in 5 cycles. The reduction of switch performance for these electrostatic complexes was attributed to the photobleaching of PT. The fluorescence switching cycle curves were plotted with the maximum fluorescence emission peak at 562 nm, and shown in Fig. 4. Although the existence of fluorescence bleaching, the fluorescence change after 5 cycles switch was still good, and it was noted that PT-DAE-3 presented the lowest bleach ratio with better photostability than the other electrostatic complexes, which made PT-DAE-3 preferable for cell imaging.

By virtue of its good fluorescence switching performance in aqueous solution, PT-DAE-3 was applied for cell imaging

experiments. PT-DAE-3 had a smaller size and better photostability, and could enter into the whole cell after incubation with MCF-7 cells for 4 h. The fluorescence switching test was performed on whole culture cells. Fig. 5a shows the good switching phenomenon in MCF-7 cells. After irradiation with UV lamp for 5 s, MCF-7 cells changed from bright to dark, and irradiation with 559 nm and 633 nm mixed laser (559/633 nm laser, mixed laser was used for the better DAE ring-open ability than single 559 nm or 633 nm laser) for 15 s, MCF-7 cells turned bright again. While there was no fluorescence switching effect observed in control group, which was treated with PT itself. After proving the fluorescence switching ability in whole cells, further the fluorescence lighting up ability of PT-DAE-3 for specific labeling of selected cells was demonstrated. Fig. 5b shows the lighting up process of selected cell among a herd of MCF-7 cells. Fig. 5b(i) depicts the quenched original fluorescence of PT-DAE-3 in the MCF-7 cells, and selected cell was irradiated with 559/633 nm laser to light up them one by one from (ii) to (viii). These results clearly show that PT-DAE-3 served as a great toggle switch for their promising potential biological imaging applications.

In summary, a facile electrostatic complex nanoparticle has been designed and prepared through mixing positively charged PT and negatively charged DAE-COONa. The average particle size of PT-DAE-3 ECNs is around 300 nm, conferring it diffusing ability toward cells and tissues. The fluorescence switching effect of this nanoparticle is excellent and it can be used in fixed cells and tissues. This electrostatic complex strategy also provides a universal method for constructing fluorescence switching system, which is an easier approach than covalent binding or reprecipitation nanoparticle method. Furthermore, the individual cell lighting up ability provides this particle with chances to be a fluorescence pen to mark cells of interest. Further, we can use some detection and separation strategy, such as flow cytometry, to collect the marked cells. We believe this electrostatic complex fluorescence switching nanoparticle will bring preparation convenience and individual cell marking ability for cell imaging.

Acknowledgments

The work described herein was supported by the National Natural Science Foundation of China (Nos. 91527306 and 21661132006), and the Strategic Priority Research Program of the Chinese Academy of Sciences (No. XDA16020804), and the Youth Innovation Promotion Association CAS (No. 2016029).

Appendix A. Supplementary data

Supplementary material related to this article can be found, in the online version, at doi:https://doi.org/10.1016/j.cclet.2019.09.019.

References

[1] D.C. Worth, M. Parsons, J. Cell Sci. 123 (2010) 3629–3638.
[2] J.T. Groves, R. Parthasarathy, M.B. Forstner, Annu. Rev. Biomed. Eng. 10 (2008) 311–338.
[3] N.S. White, R.J. Errington, Adv. Drug Deliv. Rev. 57 (2005) 17–42.
[4] T.N. Figueira, A.S. Veiga, M. Castanho, J. Mol. Struct. 1077 (2014) 114–120.
[5] G. Maulucci, A. Maiorana, M. Papi, G. Pani, M. de Spirito, Microsc. Microanal. 20 (2014) 1198–1207.
[6] M. Zhu, L. Zhu, J. Han, et al., J. Am. Chem. Soc. 128 (2006) 4303–4309.
[7] D. Hu, Z. Tian, W. Wu, W. Wan, A. Li, J. Am. Chem. Soc. 130 (2008) 15279–15281.
[8] Z. Tian, A. Li, D.H. Hu, Chem. Commun. 47 (2011) 1258–1260.
[9] F. Bonardi, G. London, N. Nouwen, B. Feringa, A.J.M. Driessen, Angew. Chem. Int. Ed. 49 (2010) 7234–7238.
[10] Q. Zhang, S.J. Rao, T. Xie, et al., Chem 4 (2018) 2670–2684.
[11] W. SzymaŃski, D. Yilmaz, A. Koçer, B.L. Feringa, Acc. Chem. Res. 46 (2013) 2910–2923.
[12] L. Ming, L.Y. Gu, Q. Zhang, M.Z. Xue, Y.G. Liu, Chin. Chem. Lett. 24 (2013) 1014–1018.
[13] L.X. Yu, Y. Liu, S.C. Chen, Y. Guan, Y.Z. Wang, Chin. Chem. Lett. 25 (2014) 389–396.
[14] Y. Zhang, K. Zhang, J. Wang, Z. Tian, A. Li, Nanoscale 7 (2015) 19342–19357.
[15] C. Xiao, W.Y. Zhao, D.Y. Zhou, et al., Chin. Chem. Lett. 26 (2015) 817–824.
[16] J.Q. Zhang, Q.C. Wang, L. Zou, C.Y. Jia, Chin. Chem. Lett. 25 (2014) 762–766.
[17] S. Yang, J. Liu, Z. Cao, et al., Dyes Pigment 148 (2018) 341–347.
[18] S. Zhu, W. Li, W. Zhu, Prog. Chem. 28 (2016) 975–992.
[19] R.M. Dickson, A.B. Cubitt, R.Y. Tsien, W.E. Moerner, Nature 388 (1997) 355–358.
[20] M. Andresen, A.C. Stiel, J. Folling, et al., Nat. Biotechnol. 26 (2008) 1035–1040.
[21] Q. Zhang, D.H. Qu, Q.C. Wang, H. Tian, Angew. Chem. Int. Ed. 54 (2015) 15789–15793.
[22] Z. Tian, W. Wu, W. Wan, A. Li, J. Am. Chem. Soc. 131 (2009) 4245–4252.
[23] Y. Zou, T. Yi, S. Xiao, et al., J. Am. Chem. Soc. 130 (2008) 15750–15751.
[24] C. Yun, J. You, J. Kim, J. Huh, E. Kim, J. Photoch. Photobiol. C -Photochem. Rev. 10 (2009) 111–129.
[25] S.E. Irvine, T. Staudt, E. Rittweger, J. Engelhardt, S.W. Hell, Angew. Chem. Int. Ed. 47 (2008) 2685–2688.
[26] F.M. Raymo, M. Tomasulo, Chem. Soc. Rev. 34 (2005) 327–336.
[27] I. Yildiz, E. Deniz, F.M. Raymo, Chem. Soc. Rev. 38 (2009) 1859–1867.
[28] G. Gao, Y.W. Jiang, W. Sun, F.G. Wu, Chin. Chem. Lett. 29 (2018) 1475–1485.
[29] Y. Chan, M.E. Gallina, X. Zhang, et al., Anal. Chem. 84 (2012) 9431–9438.
[30] T. Nakahama, D. Kitagawa, H. Sotome, et al., J. Phys. Chem. C 121 (2017) 6272–6281.
[31] Y. Zhang, K. Zhang, J. Wang, Z. Tian, A.D. Li, Nanoscale 7 (2015) 19342–19357.
[32] C.L. Zhu, L.B. Liu, Q. Yang, F.T. Lv, S. Wang, Chem. Rev. 112 (2012) 4687–4735.
[33] S. Shen, M. Mamat, S. Zhang, et al., Small 4 (2019) 1902118.
[34] C.T. Kuo, A.M. Thompson, M.E. Gallina, et al., Nat. Commun. 7 (2016) 11468.
[35] H. Chong, C. Nie, C. Zhu, et al., Langmuir 28 (2012) 2091–2098.
[36] G.M. Yang, L.B. Liu, Q. Yang, F.T. Lv, S. Wang, Adv. Funct. Mater. 22 (2012) 736–743.
[37] C.F. Xing, Q.L. Xu, H.W. Tang, L.B. Liu, S. Wang, J. Am. Chem. Soc. 131 (2009) 13117–13124.